

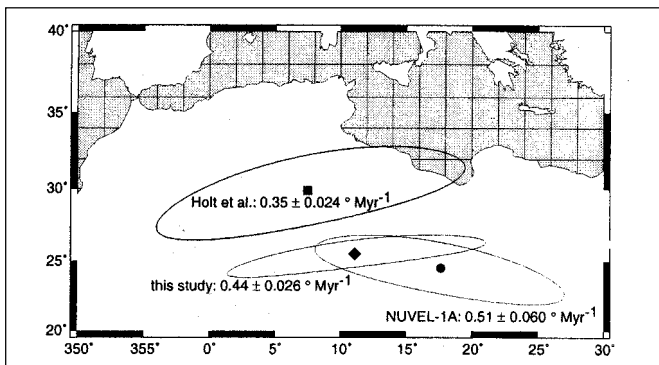
## 2. MODELLING OF GEOLOGICAL HAZARDS AND RESOURCES

### 2.1 Global Positioning System (GPS) Studies

#### 2.1.1 Crustal Deformation Studies Using GPS for Understanding the Motion and Active Deformations of the Indian Plate

Measurements of surface displacements using GPS were used to constrain the motion and deformation of Indian and Indian-Eurasian plate boundary deformations along the Himalayas. Three problems were addressed using these measurements. First, a new India-plate motion angular velocity vector was computed. The angular rotation of the Indian plate is an important quantity that provides the basic boundary conditions for the creation of all deformation features and phenomena within the Indian plate and further northward across Tibet. The geodetically constrained pole of rotation of Indian-Eurasian plate was computed to be located at  $25.6 \pm 1.0^\circ\text{N}$  and  $11.1 \pm 9.0^\circ\text{E}$  with a counterclockwise angular velocity of  $0.44 \pm 0.03$  degrees/Myr which is approximately  $6^\circ\text{W}$  of the NUVEL-1A pole of plate rotation computed from sea-floor data of the past 3 Myrs (Fig. 2.1.1.1). This is also 14% slower than the long-term NUVEL-1A angular velocity ( $0.51 \pm 0.06$  degrees/Myr). The deformation within the Indian plate was the second problem addressed and no significant strain was detected across India and it could be showed that the exposed Indian plate was stable to within  $7 \times 10^{-9}$  strain per year. Finally, regarding the deformation along the Himalayas, the first order analysis showed that the southward velocities increased from nearly

**Fig. 2.1.1.1.** Angular velocity vector poles and rates of relative motion between Eurasia and India from sea-floor data (NUVEL-1A), geodetic data (this study) and a combination of regional GPS and geologic fault slip data (Holt et. al.; J. Geophys. Res., 105, 19185-209, 2000).



zero at the foot of the Himalayas to 15-22 mm/yr north of the higher Himalayas (Fig. 2.1.1.2). The axes of maximum shortening indicated by the GPS data swings counterclockwise from  $\sim\text{N}20^\circ\text{E}$  at  $77^\circ\text{E}$  in the northwest Himalayas to  $\sim\text{N}25^\circ\text{W}$  at  $92^\circ\text{E}$  in northeastern India.

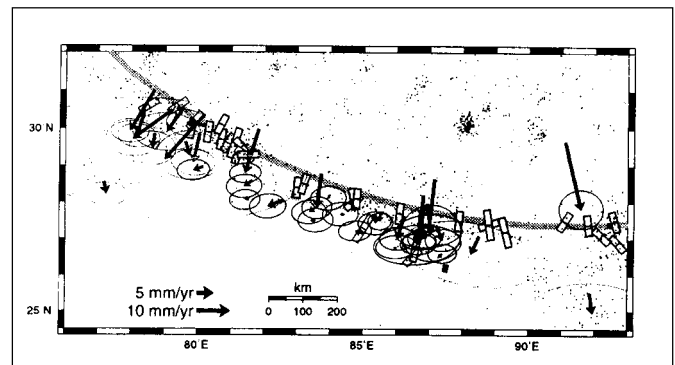
It was also significant that a southward velocity of  $6.3 \pm 3.8$  mm/yr with respect to India was measured at Shillong which is the highest intra-plate velocity recorded within the Indian plate. This implies that convergence across the Bhutan Himalayas is at least 25% slower than elsewhere in the Himalayas and also that the motion observed at Shillong could be a result of viscous adjustments near the 1897 Assam earthquake north of Shillong or the result of plateau-uplift processes. These observations have prompted plans for more detailed GPS measurements on the Shillong plateau in the near future.

(J Paul, V K Gaur, M B Ananda, Sridevi Jade, M Mukul, T S Anupama, G Satyal\* and P Dileep Kumar; \*GBPIHED, Almora)

#### 2.1.2 Deformations in the Darjiling-Sikkim Himalayas Using GPS

The next phase of the GPS work in the Himalayas is to be concentrated in the Darjiling-Sikkim Himalayas to address specific questions on the deformations in the area. As the first step, five new GPS sites have been set up and initial measurements made. The Delo Hill site (DELO -  $27^\circ 05' 21.97212''\text{N}$ ;  $88^\circ 30' 09.92233''\text{E}$ ; 1636.2 m) near

**Fig. 2.1.1.2.** GPS velocities in an Indian reference frame and maximum principal stress axes along the Himalayan arc. Convergence and stress axes across the Himalayas rotate counterclockwise by about  $45^\circ$  between  $77^\circ$  and  $92^\circ$  E longitude.



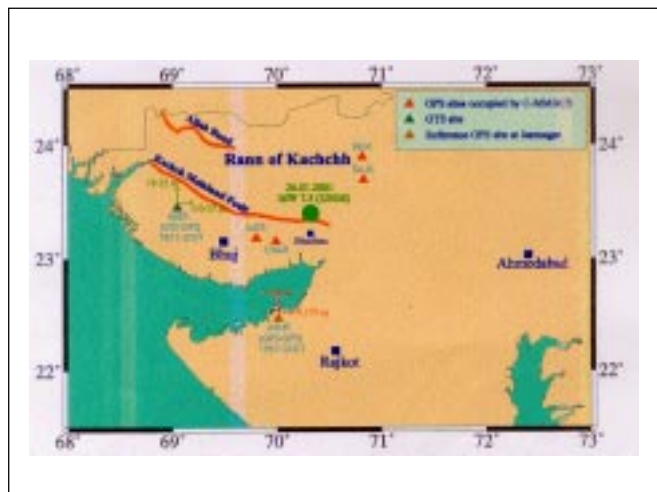
Kalimpong, West Bengal is situated in the hanging wall of the Main Central Thrust (MCT) in gneisses and is located west of a suspected active transverse zone, Gish Transverse Zone (GTZ), in the area; a near-surface, strike-slip earthquake was recorded along the trace of the GTZ (27.2°N; 88.7°E) in 1980 that suggested the presence of a transport-parallel, basin scale, active strike-slip fault in the region. To check for active deformations along the GTZ, we have put another station east of the GTZ at Siyal Pokhari near Labha, West Bengal (LABHA-27°04'12.84145"N; 88°39'48.60508"E; 1880.8 m). This site is also situated in the hanging wall of the MCT in gneisses and, along with DELO, provides GPS sites on both east and west blocks of the GTZ. To monitor possible active deformations within the basement gneisses, a GPS site has been set up at Kyongnosla near Gangtok, Sikkim (KYON-27°22'02.79187"N; 88°42'50.86997"E; 3205.1 m). This new site too is located in the hanging wall of the MCT in gneisses, but is higher in the section than the previous two sites. Preliminary fieldwork revealed that there might be two faults similar to the MCT1 and MCT2 classification in the Garhwal-Kumaon Himalayas. Then the KYON site would be in the hanging wall of the higher MCT that contains gneisses found at LABHA and DELO, in its footwall. To look at the deformations in the footwall of the MCT in the Rangit Tectonic Window (RTW), a GPS site has been established at Namchi, Sikkim (NAMCHI-27°09'25.77385"N; 88°19'17.63500"E; 1428.3 m), located in the footwall schists of the MCT. It overlies duplex structures observed in the field around Jorethang, Sikkim. Duplex structures have been suspected to be active structures elsewhere in the Himalayas; NAMCHI has been established to test this hypothesis in Sikkim. The presence of duplex structures have been inferred in the Kumaon Himalayas based on surface, seismic and borehole data, but they are well exposed in Sikkim. This makes it the ideal place to work out the kinematic implications of the duplex structures and the area around NAMCHI directly overlies this structure. Finally, a GPS site has been established at Mungpo, West Bengal (MUNG-26°58'39.32860"N; 88°24'00.03792"E; 798 m), again in the gneisses of the hanging wall of the MCT, and also in the hanging wall of the Birrik thrust, which is probably an out-of-sequence active thrust fault in the Proterozoic section of the Darjiling Himalayas as evident from geological observations such as raised river terraces, braiding of river, diversion of river channel and landslides along the Birrik fault zone.

(M Mukul, A P Krishna\*, M B Ananda, P Dileep Kumar, V K Gaur and G Satyal\*; \*GBPIHED, Almora)

### 2.1.3. Determination of the Time Evolving Surface Strain Field Around the Bhuj Area Using GPS for Estimation of the Upper Bounds of the Coseismic Displacement During the Bhuj Earthquake of January 26, 2001

The Mw 7.6 Bhuj earthquake of January 26, 2001 was felt over a wide area of the country. GPS measurements were made at seven sites (Fig. 2.1.3.1) in the epicentral tract including Jamnagar and Hathria to estimate the total residual displacements at these sites after the earthquake. GPS Coordinates of the Jamnagar site had been determined in 1997 while the Hathria and Bhuj sites had been measured 144 years ago during the Great Triangulation Survey (GTS). Comparison of GPS-GPS (1997-2001) coordinates at Jamnagar and GTS-GPS (1857-2001) coordinates at Hathria were carried out to determine the upper bounds on the displacements suffered by these sites as a result of the coseismic slip of major events that occurred in the intervening period. The displacement vector obtained at Jamnagar using GPS-GPS comparisons for the period February, 1997 - February, 2001 is 24.3168 cm at N46.3°E (Fig. 2.1.3.1). In the India reference frame, this translates to a cumulative displacement over the past four years, with respect to the permanent station at IISc, Bangalore (IISC), after accounting for the 3±2 mm/yr contraction within the Indian plate, of 16.24 mm at N34.75°E. In view of the extremely small strain rate within the Indian plate, this figure most likely represents the effect at Jamnagar of the coseismic slip on the Bhuj 2001 rupture plane.

Fig. 2.1.3.1. Displacements suffered by Jamnagar (GPS-GPS) and Hathria (GPS-GTS) sites during 1997-2001 and 1857-2001 periods respectively.



The GTS site (Hathria) in the Kutch region was measured in 1857 and includes a systematic error of 2.52' in the GTS longitude caused by the 19<sup>th</sup> century overestimation of the Madras meridian. The GTS-GPS displacement of this site over the 1857-2001 period is found to be 18.53 m (N), 116.06 m (E) after removing the systematic error in the GTS longitude and using the corrected GTS longitude of 69.04494722°N for the site. This number, however, includes the effect of steady strain accumulation in the region, coseismic slips of previous and the latest events and uncertainties in the longitude correction. However, the northern component of this displacement does give an upper bound to the northward motion suffered by this site as a result of the coseismic slip of this largest event in the region during the past 144 years.

*(Sridevi Jade, M Mukul, I A Parvez, M B Ananda, P Dileep Kumar and V K Gaur)*

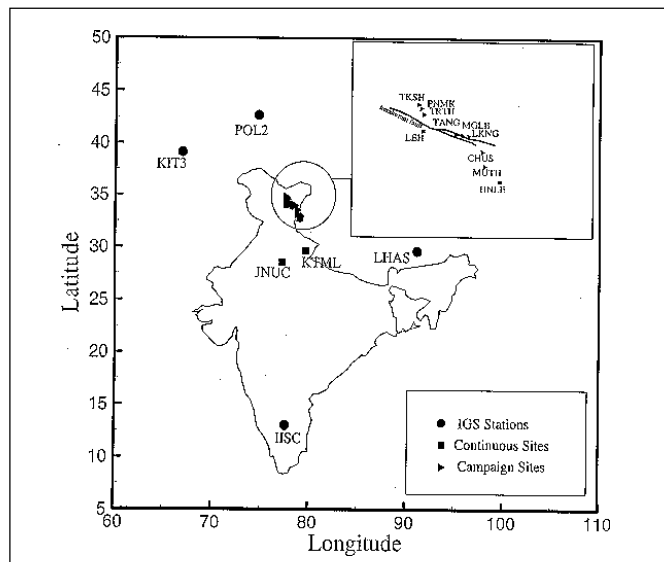
### 2.1.4 A Study of the Trans-Himalayan Kinematics in Ladakh, India

Study of trans-Himalayan kinematics in Ladakh Himalayas is based on the GPS measurements at ten to fifteen stations in Ladakh Himalayas over a period of four years (1997-2000). This region is important as it is on the Indo-Eurasian collision zone and also due to the presence of NW-SE trending Karakoram fault in northern Ladakh. The GPS derived velocities obtained in this region will give some clue regarding the convergence mechanism in the region. Ladakh GPS experiment is designed to verify whether the

convergence in this region supports the continental deformation model of, (1) crustal thickening and shortening in the Himalayas, (2) internal thickening and shortening within the Tibetan plateau, (3) limited crustal shortening across the northern, northeastern and eastern margins of the Tibetan plateau or, (4) the eastward extrusion of Tibet and southeast Asia away from the indenting Indian plate. The sites occupied in the 4-year period during the Ladakh GPS Campaign are shown in Fig. 2.1.4.1. The figure also shows four sites- Delhi (JNUC), Almora (KTML), Leh (LEH) and Hanleh (HNLE)- which were run continuously throughout the Ladakh campaign period and four IGS sites- Bangalore (IISC), Kitab (KIT3), Pol2 (POL2) and Lhasa (LHAS)- which were used in the analysis. The campaign data have been processed along with the GPS data of the four GPS global tracking network sites referred to as IGS (International GPS service for Geodynamics) sites, using Bernese software. The coordinates and the baseline lengths between the stations are estimated by constraining the IGS station coordinates to their predetermined values. Rates of baseline shortening between IISC and the rest of the stations and the absolute velocities of these sites are estimated by constraining the IISC coordinates to its value in the International Terrestrial Reference Frame 1996 (ITRF96) reference frame.

The GPS absolute velocity vectors are shown in Fig. 2.1.4.1. The values obtained make possible a discussion on the trans-Himalayan kinematics in this region based on the GPS studies which is first of its kind in this region. The results are also compared with the available kinematic rates of shortening, extension and strike slip fault motion in this region. The significant results to be inferred from the GPS velocity vectors are as follows. Rates of baseline shortening between IISC-JNUC and IISC-KTML are negligible. In other words, Bangalore, Delhi and Almora have almost the same absolute velocities which substantiate the fact that Delhi and southern Himalayas (Almora) are locked to Indian plate and move along with it. Rates of baseline shortening between IISC and the sites in Ladakh Himalayas range from 14-20 ( $\pm 4$ ) mm/yr. This is consistent with the crustal shortening rates in Himalayas. Rates of baseline shortening between IISC-KIT3 ( $27.52 \pm 4.69$  mm/yr) and IISC-POL2 ( $33.65 \pm 5$  mm/yr) give an indication of the movement on the strike slip Chaman Fault. The rate of baseline shortening between IISC-LHAS ( $15.16 \pm 4$  mm/yr) is also consistent with the convergence rates in the eastern Himalayas. The GPS derived velocities of the IGS stations, Bangalore, Kitab, Pol2 and Lhasa, are consistent with the IGS-GPS derived velocities. The velocities of the Ladakh Himalaya sites with respect to Lhasa indicate that there is E-W

Fig. 2.1.4.1. GPS derived absolute velocity vectors (1997-2000) of the GPS sites in Ladakh Himalayas alongwith the IGS stations.



extension between these sites and Lhasa at a rate of 15mm/yr oriented N72°W. The sites in Ladakh Himalayas move S-W with respect to Bangalore at a rate of 19 mm/yr oriented S28°W. The velocities of sites in Ladakh Himalayas with respect to Leh indicates the strike slip motion on the Karakoram fault; the results indicate a small right lateral slip on the Karakoram fault.

(*Sridevi Jade, V K Gaur, M B Ananda, B C Bhatt\* and P Dileep Kumar; \*IIA, Ladakh*)

## 2.2. Microtectonics in the Neotectonically Active Part of the Himalayan Wedge: Deformation Mechanisms in the South Kalijhora Thrust and Thrust Sheet in Darjiling Himalayan Fold-and-Thrust Belt, West Bengal, India

Previous work in the Darjiling-Sikkim-Tibet (DaSiT) Himalayan wedge at C-MMACS revealed that the middle part of the wedge is the location for neotectonic deformation as evident from earthquake hypocenter data and geologic evidence. Microtectonic studies in this part of the wedge were carried out to look at the deformation signatures in the rocks to understand the kinematics of deformation at the microscopic level and their implications. The rocks of the South Kalijhora thrust (SKT) sheet in the footwall of the Main Boundary thrust (MBT) were studied for this purpose. The SKT is a footwall imbricate of the MBT and is well exposed along a ramp in a section of the Tista River valley in the Darjiling Himalayan fold-and-thrust belt.

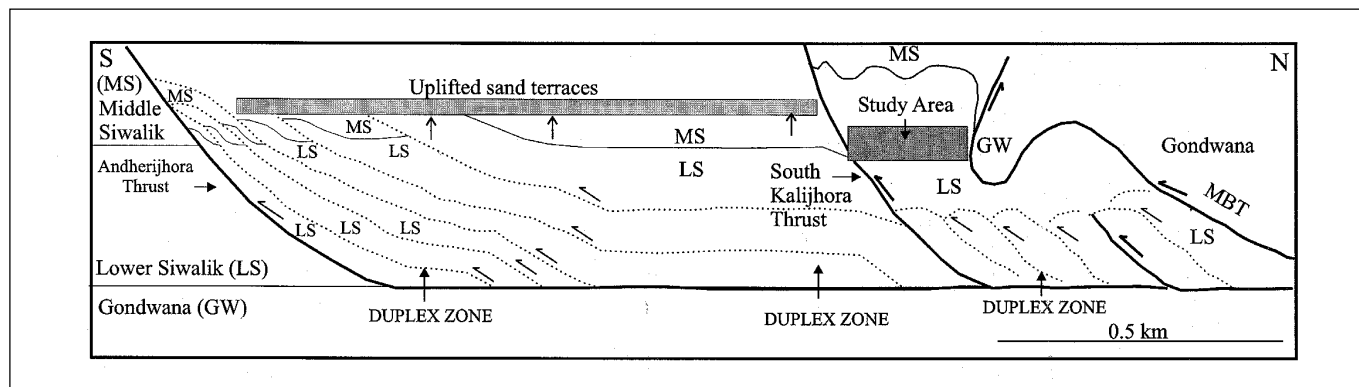
There are three distinct deformation events that affect the rocks of the SKT sheet; these are shown in Fig. 2.2.1. First, the development of the fault-propagation fold pair during the propagation of the SKT; the MBT was folded

during the propagation of the SKT into a fault-propagation antiform and synform. Second, the low-angle breakthrough of the SKT through the fault-propagation structure, preserving the folds in its hanging wall, and ramp formation with fault-parallel shear deformation in the SKT fault zone. Finally, re-activation of the DaSiT wedge caused the formation of connective splay duplexing in the region. Each of these deformation events seem to have left distinct signatures in the deformation microstructures observed in the rocks of the SKT sheet.

The fault-propagation-folding event occurred under quasi-plastic conditions as evident from the deformation microstructures developed in the quartz grains from the sandstone in the SKT sheet. Near the MBT, the quartz grains exhibit undulose extinction and deformation bands (Fig. 2.2.2) along with recovery microstructures indicating that dislocation creep was the dominant quasi-plastic deformation mechanism in the SKT sheet near the MBT fault zone. However, only undulose extinction is seen in quartz grains from fold hinges near the SKT fault zone, and no recovery microstructures are observed indicating that dislocation glide is the only quasi-plastic deformation mechanism that is operative. Also, the quasi-plastic deformation in the quartz grains decreases away from the MBT fault zone and there is an increase in the frequency of quartz grains with straight extinction.

In the SKT fault zone, the fine-grained matrix of the conglomerate unit exhibit schistosity and folding whereas the clasts exhibit shear fracturing (Fig. 2.2.3). Lignite boulders in the SKT fault zone, however, exhibit flow around other clasts. In the SKT sheet, elastically-frictional deformation dominates near the SKT fault zone. Carbonate and sericite filled fractures (Fig. 2.2.4) are typically associated with SKT sheet rocks close to the SKT fault zone. The frequency of these fractures decrease away from

**Fig. 2.2.1.** Cross-section of the study area showing the major faults and the thrust sheets in the area. The Main Boundary Thrust (MBT) was folded by the propagation of the SKT.



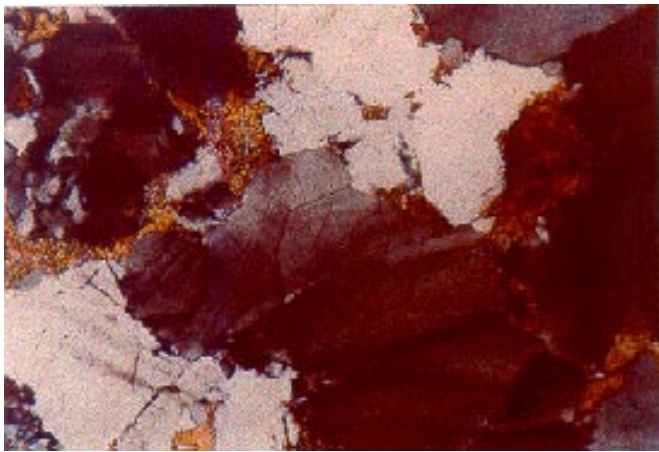


**Fig. 2.2.2.** Undulose extinction and deformation bands in quartz grains of Chunabati sandstone in the SKT sheet near the MBT fault zone. This indicates that dislocation creep was the dominant quasi-plastic deformation mechanism in the SKT sheet near the MBT fault zone. Width of the photomicrograph is 1.95 mm.

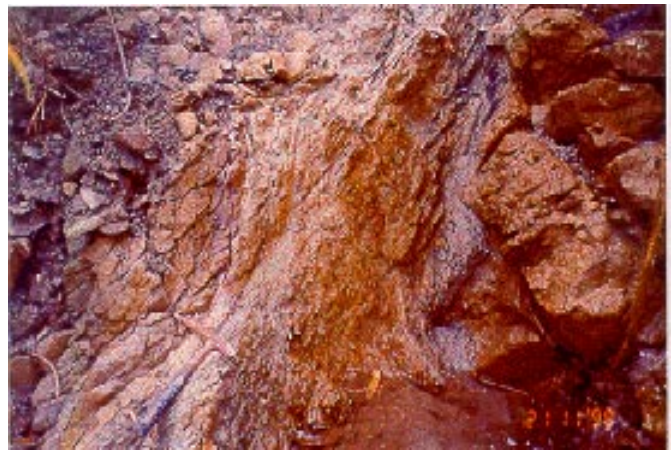


**Fig. 2.2.3.** Grain-size dependent deformation mechanisms in the SKT fault zone conglomerate. The larger clasts have fractures by fault related shearing whereas the finer grained matrix exhibits schistosity and flow. Presence of lignite as part of the fine grained matrix is evident from black strands in the matrix, the best example of which is seen near the fractured clasts above the hammer (for scale). The hanging wall sandstones are seen to the right of the photograph defining the hanging wall cut-off.

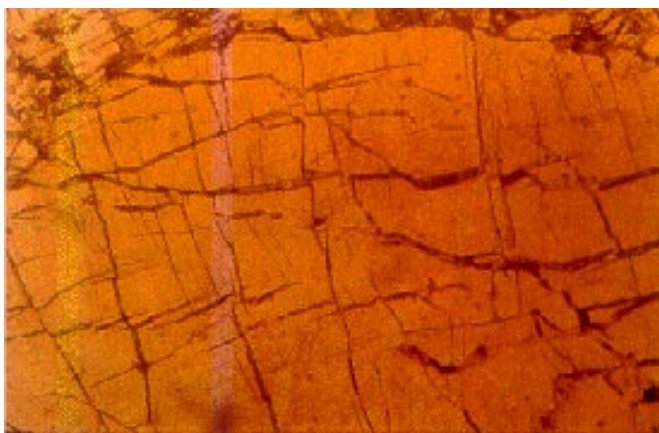


**Fig. 2.2.4.** Carbonate and sericite filled, possibly cleavage-controlled, fracturing in a K-Feldspar grain from the Chunabati sandstones in the SKT sheet. These fracturings also exhibit enechelon patterns at places and overprint earlier, randomly oriented healed fractures which show up as faint lines in the background of the photomicrograph.

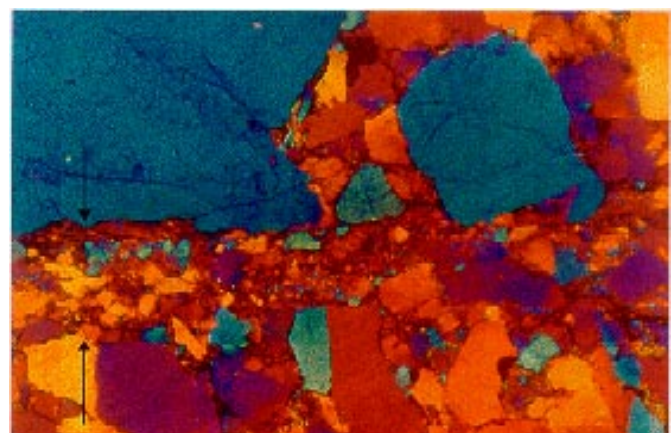


**Fig. 2.2.5.** Cemented cataclasite zone in Chunabati sandstones from the SKT sheet near the SKT fault zone. Most quartz grains exhibit little or no undulose extinction suggesting limited quasi-plastic deformation in the rock near the SKT fault zone. Randomly oriented intragranular healed fractures are seen to be overprinted by later intragranular and transgranular fractures in the large quartz grains above the cataclasite zone.

the SKT fault zone indicating that these microfractures are, in all probability, associated with the deformation in the SKT fault zone. The quasiplastic deformation features in quartz grains and the filled-fractures are overprinted by mostly transgranular fracturing and cataclasis (Fig. 2.2.5) that are probably associated with the duplex formation in the area.

geological time-scales) from quasi-plastic during the initial stages of propagation of the SKT to elasto-frictional by the time the SKT ramped upsection. This points to fairly rapid erosion in the DaSiT wedge over the SKT sheet which, as postulated earlier, probably led to the duplex formation subsequently in the wedge.

The above observations point to the fact that the deformation mechanisms changed fairly rapidly (in

*(M Mukul and K Basak\*, \*Calcutta University)*